

Fault Diagnosis of Rolling Element Bearings with a Spectrum Searching Method

Wei Li¹, Bo Wu¹, Zhencai Zhu¹, Mingquan Qiu¹, and Gongbo Zhou¹

¹School of Mechanical Engineering,
China University of Mining and Technology,
Xuzhou, 221116, P.R. China. Email: liwei_cmee@163.com

Abstract

Rolling element bearing faults in rotating systems are observed as impulses in the vibration signals, which are usually buried in noises. In order to effectively detect the fault of bearings, a novel spectrum searching method is proposed. The structural information of spectrum (SIOS) on a predefined basis is constructed through a searching algorithm, such that the harmonics of impulses generated by faults can be clearly identified and analyzed. Local peaks of the spectrum are located on a certain bin of the basis, and then the SIOS can interpret the spectrum via the number and energy of harmonics related to frequency bins of the basis. Finally bearings can be diagnosed based on the SIOS by identifying its dominant components. Mathematical formulation is developed to guarantee the correct construction of the SIOS through searching. The effectiveness of the proposed method is verified with a simulation signal and a benchmark study of bearings.

Keywords: Fault diagnosis, Bearings, Spectrum, Searching method

1 Introduction

Rotating machinery is widely used in many industrial fields. Fault diagnosis in rotating machinery is important for system maintenance and process automation. In practice, faulty bearings contribute to most of the failures in rotating machinery [1, 2, 3, 4]. It is reported that approximately 90% of rolling element bearing failures are related to either inner-race or outer-race flaws [5]. Periodic sharp impulses characterize these faults, and the characteristic frequencies can be theoretically computed. Nevertheless those impulses are of low energy and usually buried by noises. These signals are usually modulated by some high-frequency harmonic components and resulted in a series of harmonics of characteristic frequencies [2].

In order to realized fault diagnosis of bearing, usually some features of vibration signals are extracted through time-domain methods, frequency-domain methods, and time-frequency methods [3]. Time-domain methods are directly based on the time waveform, e.g. peak amplitude, root-mean-square amplitude, variance, skewness, kurtosis, correlation dimension and fractal dimension. Frequency-domain methods are based on the transformed signal in frequency domain, i.e. Fourier spectrum, cepstrum analysis, envelope spectrum. Wavelet analysis, short time Fourier transform, Wigner-Ville distribution and Hilbert-Huang transform are the time-frequency methods [6, 7], which investigate waveform signals in both time and frequency domain. When used to analyze noisy bearing vibration signals, most of those methods may produce unsatisfactory results and may not give useful information about the characteristic frequencies in order to identify the faults.

Spectrum kurtosis [8] was developed to identify the characteristic frequencies of bearings, where a filter was designed to get the signal with the maximum kurtosis in spectrum and then the envelope analysis was usually applied to show the characteristic frequencies. The wavelet techniques were widely used to decompose the vibration signals in order to find the most useful filter for fault diagnosis [9, 10, 11]. The conventional band-pass filters were also applied whose parameters were optimized through genetic algorithms or adaptive algorithms [12, 13]. Those methods are relatively complex which involve complicate computations.

Indeed spectrum kurtosis based methods are to find the resonant frequency band of vibration signals which contains a train of high-energy harmonics of characteristic frequency, and then transform the resonant frequency band to a low frequency band through envelope analysis. It is suggested that the characteristic frequency could be identified by finding harmonics with high energies in spectrums. References [2] also pointed out that the impulses of bearing faults could be detected when a series of harmonics of the characteristic frequency are identified in the spectrums.

This paper proposes a simple method to detect the faults in bearings by searching the dominant harmonics in spectrums. As discussed before, the impulses generated by bearing faults are usually modulated, and harmonics of the bearing characteristic frequency can be found in the spectrum of vibration signals. Hence we simply search the local peaks in the spectrum of vibration signals. Then the local peaks related to harmonics of certain frequency is located on a predefined basis, such that the so-called structure information of the spectrum (SIOS) of the spectrum is constructed. The SIOS includes two defined indexes, which provide the information about the number and the energy of harmonics of certain frequency. The dominant component in the SIOS is just corresponding to the characteristic frequency of bearings and therefore the bearing faults can be diagnosed.

The rest of the paper is organized as follows. Section 2 introduces the spectrum searching method and the SIOS. In section 3, the method is applied to diagnose bearing with a simulated signal, and then it is compared with a benchmark study. The discussion and concluding remarks are given in section 4 and section 5.

2 Spectrum Searching Method

As illustrated in [2], faults of rolling element bearings generate impulses, and excites frequency resonances of the whole structure between the bearing and the transducer. The low harmonics of the bearing characteristic frequencies are usually masked by other vibration components; while the harmonics can be found easier in a higher frequency range, but higher harmonics may smear over one another. In case of heavy noises the harmonics series usually can not be directly recognized in the spectrum. The harmonics do exist in the spectrum, but it is not possible to determine the bearing characteristic frequencies by measuring the spacing of the harmonic series. Hence we propose the spectrum searching method to identify the bearing characteristic frequencies. The main steps are as follows:

- find the local peaks with locally larger amplitudes in the spectrum by searching over the whole frequency range,
- construct the SIOS on the pre-defined basis by relating local peaks to frequency bins of the basis, and
- identify the dominant frequency on the basis according to the SIOS.

In this section we will describe the first two steps. For convenience in the rest of the paper, $P(k)$ is defined as the amplitude of the k th frequency bin in the spectrum; $F(k)$ is defined as the frequency in Hz corresponding to the k th frequency bin; and $I(k)$ is defined to indicate whether the k th frequency bin has a local peak or not. The resolution of the spectrum is denoted as Δ_s .

2.1 Find the Peaks in the Spectrum

The spectrum consists of the power amplitude of each frequency bin. In order to construct the SIOS, we define the local peaks of the spectrum as follows.

Definition of Local Peaks. Given three frequency bins of the spectrum, i.e. $F(k-1)$, $F(k)$ and $F(k+1)$, then $P(k)$ is called a local peak if

$$P(k) > P(k-1) \text{ and } P(k) > P(k+1). \quad (1)$$

By searching on the spectrum, all frequency bins satisfying Eq. (1) can be found. Fig. 1 gives an example of local peaks.

Such a definition may leads to a large number of local peaks. Obviously we are not interested in the frequency bins with small amplitudes with respected to noises. The harmonics of bearing characteristic frequencies are usually with relatively larger amplitudes. Hence a threshold is proposed to suppress the influence of noises to some extent as follows

$$J_{th}(k) = \frac{1}{2l+1} \sum_{i=k-l}^{k+l} P(i) + \delta, \quad (2)$$

where l and δ are nonnegative constants. If $P(k)$ satisfies Eq. (1) and

$$P(k) > J_{th}(k), \quad (3)$$

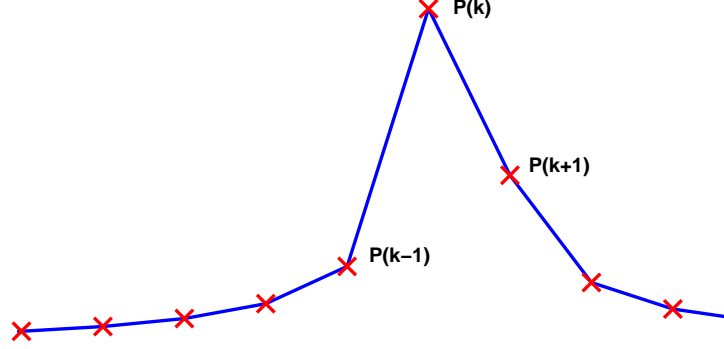


Figure 1: An example of local peaks.

then

$$I(k) = 1,$$

and otherwise

$$I(k) = 0$$

The threshold in Eq. (2) is varying in terms of k . The first part of the threshold is the moving average of power amplitudes; and the second part, i.e. δ , is used to control the total number of identified local peaks.

Fig. 2 depicts a power spectrum of a rolling element bearing with an inner-race fault. The threshold is selected with $l = 25$ and $\delta = 0.0045$, such that 2000 peaks are found.

2.2 Construct the SIOS

Assume the bearing characteristic frequencies are within the range from F_l to F_h in Hz (F_l and F_h are both bins in the spectrum), and a basis is defined as

$$B = [F_l, F_l + \Delta_B, F_l + 2\Delta_B, F_l + 3\Delta_B, \dots, F_h]$$

where Δ_B is a positive constant. Therefore the number of frequency bins of B is $(F_h - F_l)/\Delta_B$. We use $B(i)$ to represent the i th frequency bin of B . Δ_B is suggested to be the resolution of the spectrum or its demultiplier, and we denote it as

$$\Delta_B = \frac{\Delta_s}{\theta}, \theta \text{ is a positive integer.}$$

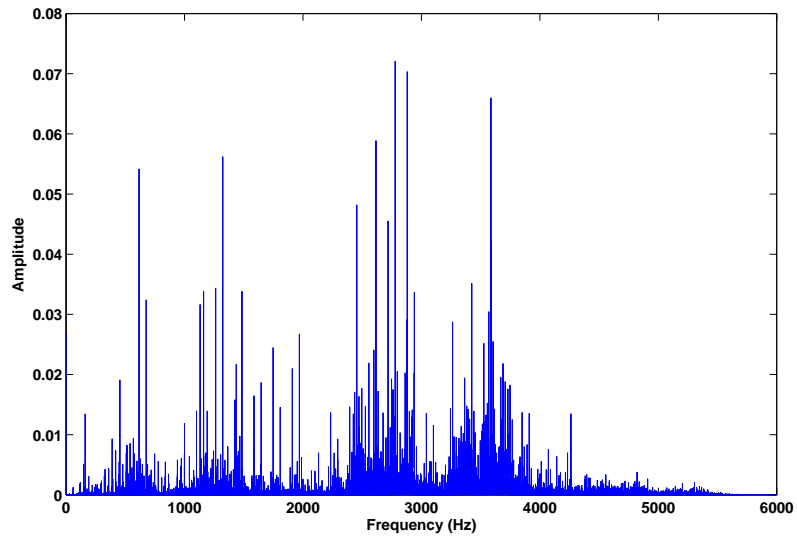


Figure 2: The spectrum of a rolling element bearing.

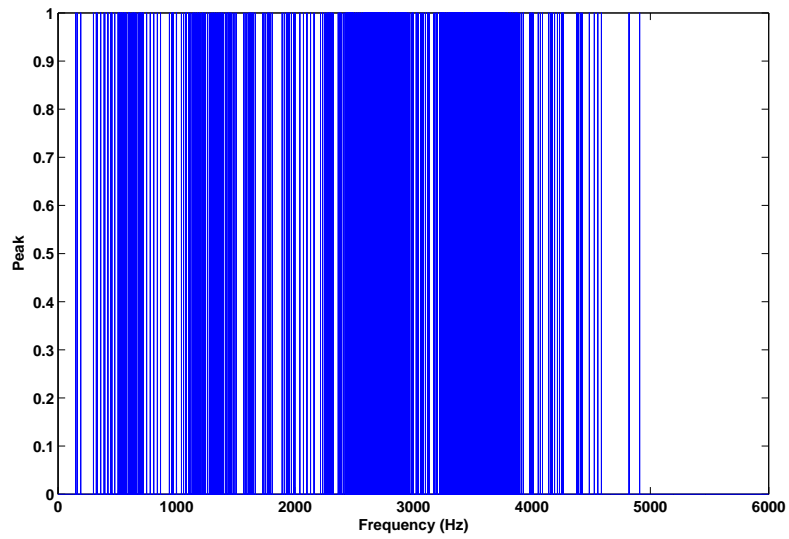


Figure 3: The peaks found in the spectrum shown in Fig. 2.

We define two indexes to represent the SIOS. The first one is the number of local peaks belonging to the i th bin on B , i.e. $N(i), i = 1, 2, \dots, (F_h - F_l)/\Delta_B$. If a local peak is found on the k th frequency bin of the spectrum, then it is located on the i th bin of B if

$$F(k)/B(i) \text{ is an integer.} \quad (4)$$

Hence we have

$$N(i) = \sum I(k), \text{ where } B(i) \text{ and } F(k) \text{ satisfy Eq. (4).}$$

If $F(k)$ is located on a bin of B according to Eq. (4), then the harmonics of $F(k)$ will also be located on the same bin.

The second index is the total energy of local peaks located on the i th bin of B , i.e. $E(i), i = 1, 2, \dots, (F_h - F_l)/\Delta_B$, and

$$E(i) = \sum P(k), \text{ where } B(i) \text{ and } F(k) \text{ satisfy Eq. (4).}$$

This index is used to distinguish the useful signal from the noises. If $B(i)$ is corresponding to a characteristic frequency of bearings, $E(i)$ should be relatively large.

In case the characteristic frequency of bearings and its harmonics are multipliers of the i th frequency bin of B , all of them should be located on the i th bin of B . Then the corresponding $N(i)$ and $E(i)$ could be a dominant component in the SIOS. Nevertheless the interval of the basis and the resolution of the spectrum can not be infinitely small. Hence the characteristic frequency of bearings and its harmonics may not be the frequency bins of the spectrum, and they may also not be located on the bin of the basis according to Eq. (4). For instance a given frequency, f_m , within the range of B described by

$$f_m = \alpha_{B(i)}\Delta_B + b_B, F_l \leq \alpha_{B(i)}\Delta_B = B(i) \leq F_h, 0 \leq b_B < \Delta_B \quad (5)$$

can not be located on B when $b_B \neq 0$, where $\alpha_{B(i)}$ is a positive integer and the term $\alpha_{B(i)}\Delta_B$ is the i th bin of B . The j th harmonic of f_m denoted by

$$\beta_j f_m$$

may also not be located on B , where $\beta_j = j$.

In order to overcome this problem, we reformulate Eq. (4) as

$$\beta_j f_m/B(i) - \lfloor \beta_j f_m/B(i) \rfloor < \sigma, \quad (6)$$

where $\sigma > 0$ and $\lfloor \cdot \rfloor$ is the flooring operator. Without loss of generality, f_m is set as

$$P(k) \leq f_m < P(k+1)$$

or

$$P(k-1) < f_m \leq P(k).$$

We would like to find σ in Eq. (6), such that f_m and its harmonics are all located on the i th bin of B when Eq. (1), (3) and (6) are satisfied.

Firstly considering the limitation of interval of the basis, we have

$$\frac{\beta_j f_m}{\alpha_{B(i)}\Delta_B} = \frac{\beta_j(\alpha_{B(i)}\Delta_B + b_B)}{\alpha_{B(i)}\Delta_B} = \beta_j + \frac{\beta_j b_B}{\alpha_{B(i)}\Delta_B}.$$

It is clear that, the frequency represented by Eq. (5) is not located on a bin of the basis when $\frac{\beta_j b_B}{\alpha_{B(i)}}$ is not a multiplier of Δ_B . Since $0 \leq b_B < \Delta_B$, we have

$$\frac{\beta_j f_m}{\alpha_{B(i)} \Delta_B} = \beta_j + \frac{\beta_j b_B}{\alpha_{B(i)} \Delta_B} < \beta_j + \frac{\beta_j}{\alpha_{B(i)}}. \quad (7)$$

Secondly considering the finite resolution of the spectrum, the given frequency f_m can also be described in terms of spectrum resolution as follows

$$f_m = \alpha_s \Delta_s + b_s$$

where α_s is a positive integer, and $0 \leq b_s < \Delta_s$. Then we have

$$\begin{aligned} & \frac{\beta_j (\alpha_s \Delta_s + b_s)}{\alpha_{B(i)} \Delta_B} \\ &= \frac{\beta_j (\alpha_s \theta \Delta_B + b_s)}{\alpha_{B(i)} \Delta_B} \\ &= \frac{\beta_j (\alpha_{B(i)} \Delta_B + b_s)}{\alpha_{B(i)} \Delta_B} \\ &= \beta_j + \frac{\beta_j b_s}{\alpha_{B(i)} \Delta_B}. \end{aligned}$$

Since $0 \leq b_s < \Delta_s$, then

$$\frac{\beta_j f_m}{\alpha_{B(i)} \Delta_B} = \beta_j + \frac{\beta_j b_s}{\alpha_{B(i)} \Delta_B} < \beta_j + \frac{\beta_j \theta \Delta_B}{\alpha_{B(i)} \Delta_B} = \beta_j + \frac{\beta_j \theta}{\alpha_{B(i)}}. \quad (8)$$

Assume $\beta_j \theta$ is smaller than $\alpha_{B(i)}$ (**Assumption 1**), then $0 \leq \frac{\beta_j}{\alpha_{B(i)}} < 1$ in Eq. (7) and $0 \leq \frac{\beta_j \theta}{\alpha_{B(i)}} < 1$ in Eq. (8). By setting

$$\sigma = \frac{\beta_j \theta}{\alpha_{B(i)}},$$

we have

$$\frac{\beta_j f_m}{\alpha_{B(i)} \Delta_B} - \lfloor \frac{\beta_j f_m}{\alpha_{B(i)} \Delta_B} \rfloor < \sigma$$

according to Eq. (7) and (8). Clearly f_m and its harmonics can be located on the same bin on $B(i)$.

The assumption 1 made on $\beta_j \theta$ and $\alpha_{B(i)}$ can generally be satisfied. The parameter β_j in Eq. (5) is constrained by

$$\beta_j \leq \frac{\text{sample rate}}{2f_m}.$$

For a given spectrum and basis, $\alpha_{B(i)}$ becomes larger when θ is larger, as

$$\frac{F_l}{\Delta_B} = \frac{\theta F_l}{\Delta_s} \leq \alpha_{B(i)} \leq \frac{\theta F_h}{\Delta_s} = \frac{F_h}{\Delta_B}.$$

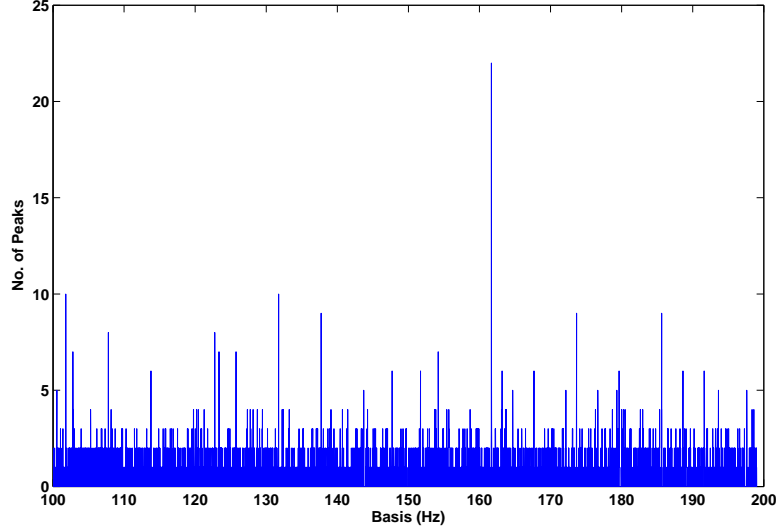


Figure 4: The number of local peaks on the basis of the spectrum in Fig. 2.

Hence when the sampling length is sufficient large, the spectrum resolution could be small enough such that

$$\Delta_s < \frac{1}{\beta_j}.$$

Then we have

$$\alpha_{B(i)} \geq \frac{\theta F_l}{\Delta_s} > \beta_j \theta F_l$$

and

$$\frac{\beta_j \theta}{\alpha_{B(i)}} < \frac{1}{F_l}$$

If $F_l > 1\text{Hz}$, then the assumption 1 is satisfied. For instance, we are interested in $f_m = 120\text{Hz}$ and its $60\times$ harmonic, i.e. $\beta_j \leq 60$, while the sampling rate and the sampling length is 12000Hz and 2^{15} respectively. Then

$$\frac{\beta_j \theta}{\alpha_{B(i)}} = 0.4392 < 1$$

with $F_l = 100\text{Hz}$, $\theta = 10$.

In Fig. 4 and Fig. 5, $N(i)$ and $E(i)$ of Fig. 2 are displayed. The SIOS, i.e. $N(i)$ and $E(i)$ on B , clearly gives the information about the harmonics of the frequency bins of B . The index $N(i)$ represents the number of harmonics of $B(i)$ found in the spectrum; and the index $E(i)$ represents the total energy of harmonics of $B(i)$. In fact the spectrum is interpreted in terms of $B(i)$, $N(i)$ and $E(i)$. It can be observed from Fig. 4 and Fig. 5, the dominant frequencies found with $N(i)$ and $E(i)$ conform with each other. Hence whether the dominant frequency identified by $N(i)$ is corresponding to a fault or not, can be further verified with $E(i)$ by looking at the energy of the dominant frequency.

In next a simulation and a benchmark study are used to describe how to realize bearing diagnosis using the SIOS.

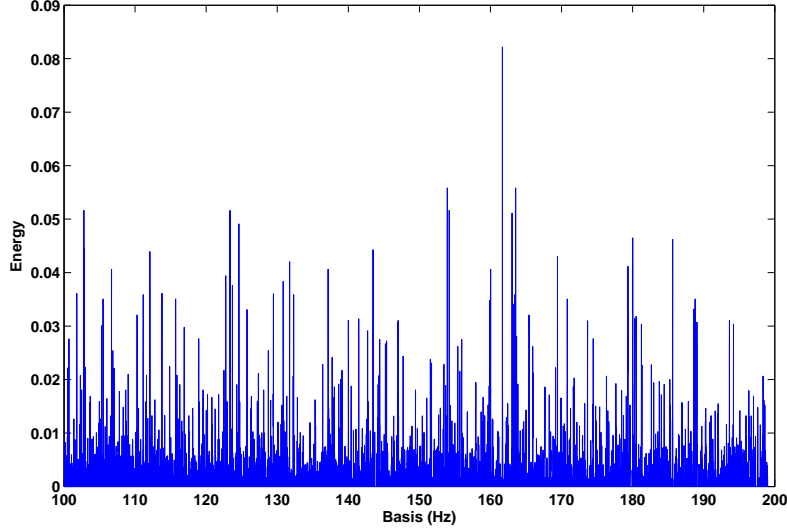


Figure 5: The total energy of local peaks on the basis of the spectrum in Fig. 2.

3 Detection of characteristic frequencies of faulty bearings by identifying the dominant frequency

3.1 Simulated bearing fault signals with one resonant frequencies

In order to demonstrate the proposed method, we use the similar simulated bearing fault signals that given in [9, 12]. The simulated bearing fault signal with one resonant frequency is given as:

$$x(k) = \sum_r \exp^{-\beta \times (k - r \times F_s / f_m - \tau_r) / F_s} \times \sin(2\pi f \times (k - r \times F_s / f_m - \tau_r) / F_s)$$

where β is equal to 900, f_m is the fault characteristic frequency ($f_m = 110\text{Hz}$), F_s is the sampling frequency ($F_s = 12000\text{Hz}$), τ_r is a uniformly distributed random number which is used to simulate the randomness caused by the slippage, and f is the resonant frequency ($f = 3900\text{Hz}$). Gaussian noise is also added and the signal noise ratio is set as -20dB .

It is known that the slippage of bearings cause smearing of harmonics. In this case the power amplitudes of harmonics will be distributed to adjacent bins. Such effects will definitely influence the diagnosis results. Therefore we consider two cases: (a) $\tau_r \in [-2, 2]$; (b) $\tau_r \in [-4, 4]$. The original signals are shown in Fig. 6 and Fig. 7, where only 500 samples are displayed.

The SIOS in case of (a) is given in Fig. 8 and Fig. 9, and in case of (b) is given in Fig. 10 and Fig. 11, where the basis is selected as $[100\text{Hz}, 200\text{Hz})$ with the interval being $0.1 \times \Delta_s$. It is clear that, when slippage is larger, the fault

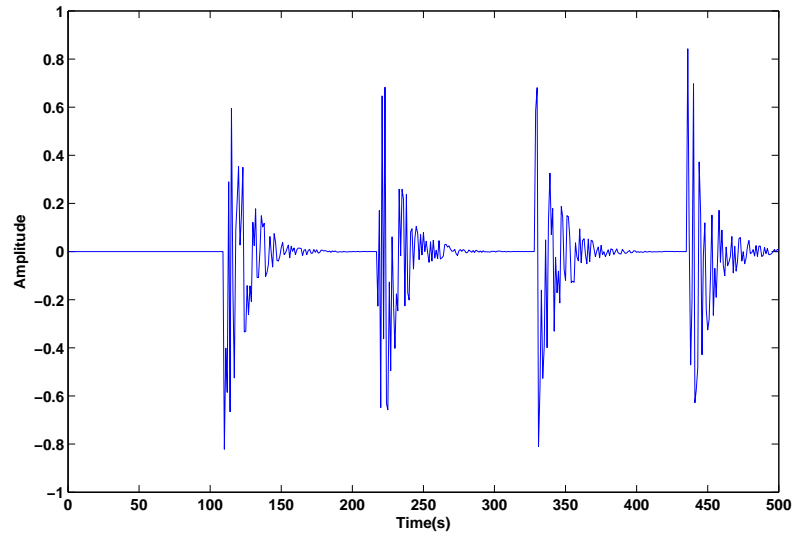


Figure 6: The simulated signal: case (a).

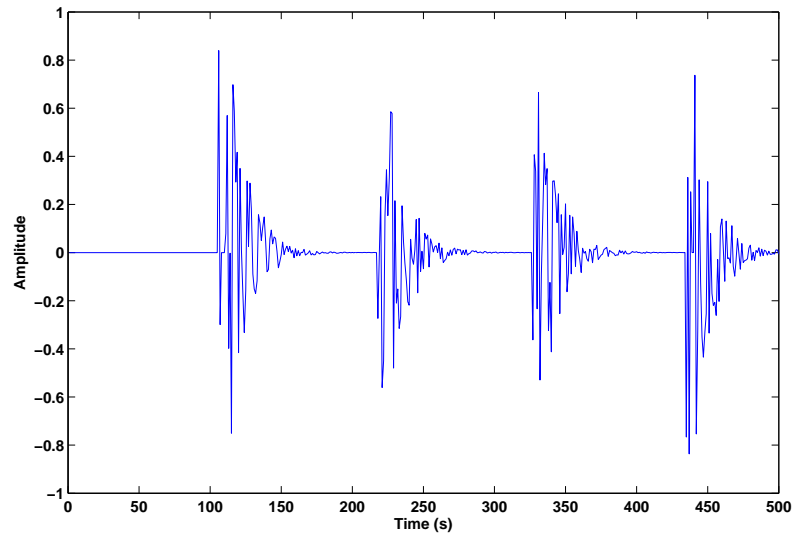


Figure 7: The simulated signal: case (b).

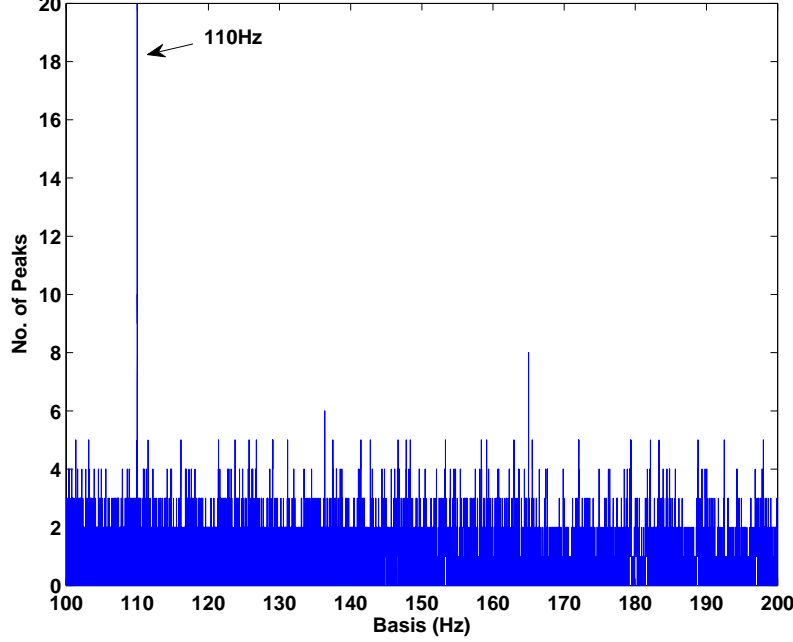


Figure 8: The SIOS of the simulated signal: $N(i)$ in case of (a).

characteristic frequency become difficult to detect. As shown in Fig. 12 almost no evident frequency bins, which are related to the fault characteristic frequency, can be found in the spectrum (case of (b)). The power amplitudes of harmonics are significantly reduced due to smearing. However the proposed method is still effective as shown in Fig. 10 and Fig. 11, where f_m is clearly identified. The main reason is that, the SIOS gives information about all harmonics even with small amplitudes through the searching algorithm.

3.2 Bearing fault signals from a benchmark study

The vibration data from the Case Western Reserve University (CRWU) Bearing Data Center [14] are analyzed and compared with the published benchmark results in [15]. The test stand consists of a 2 hp motor (left), a torque transducer/encoder (center), a dynamometer (right), and control electronics. The test bearings support the motor shaft. With the help of electrostatic discharge machining, inner-race and outer-race faults of different sizes are made. The vibration data are collected using accelerometers attached to the housing with magnetic bases. In this study, the driver end (DE) data with the sampling frequency being 12,000 Hz are analyzed. The characteristic frequencies of bearings, i.e. ball pass frequency of outer-race (BPFO), ball pass frequency of inner-race (BPFi), fundamental train frequency (FTF) and ball spin frequency (BSF), are shown in Table 1. And we use f_r to denote the rotating frequency.

The basis is selected as [100Hz, 180Hz), and $\Delta_B = 0.1\Delta_s$, $\sigma = 0.0002$ (0.002 is used for records 3005 - 3008), $l = 10000$ for all records. We firstly take records

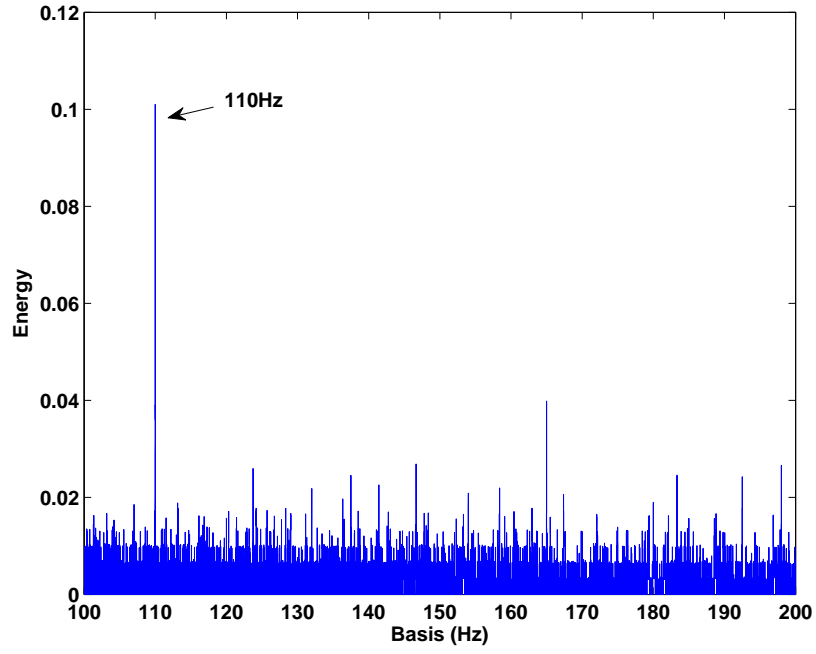


Figure 9: The SIOS of the simulated signal: $E(i)$ in case of (a).

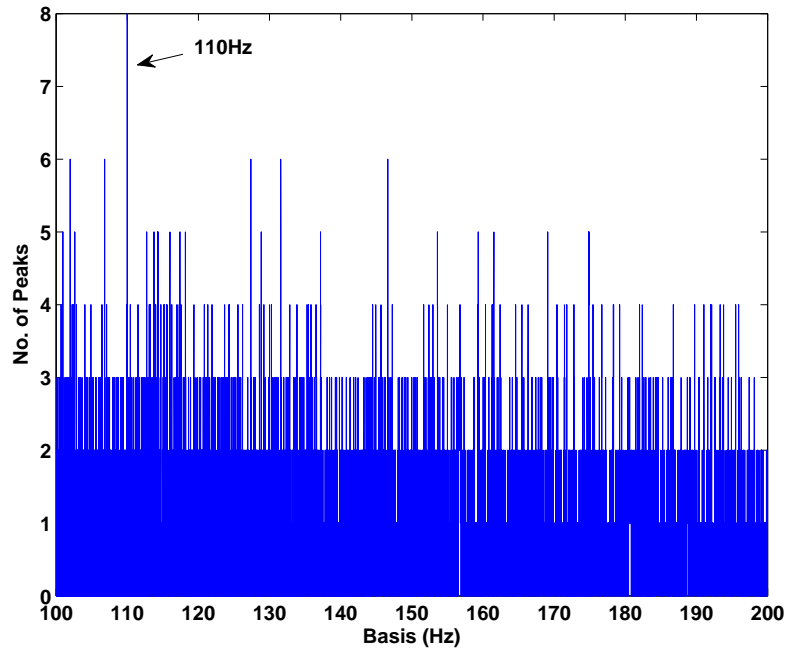


Figure 10: The SIOS of the simulated signal: $N(i)$ in case of (b).

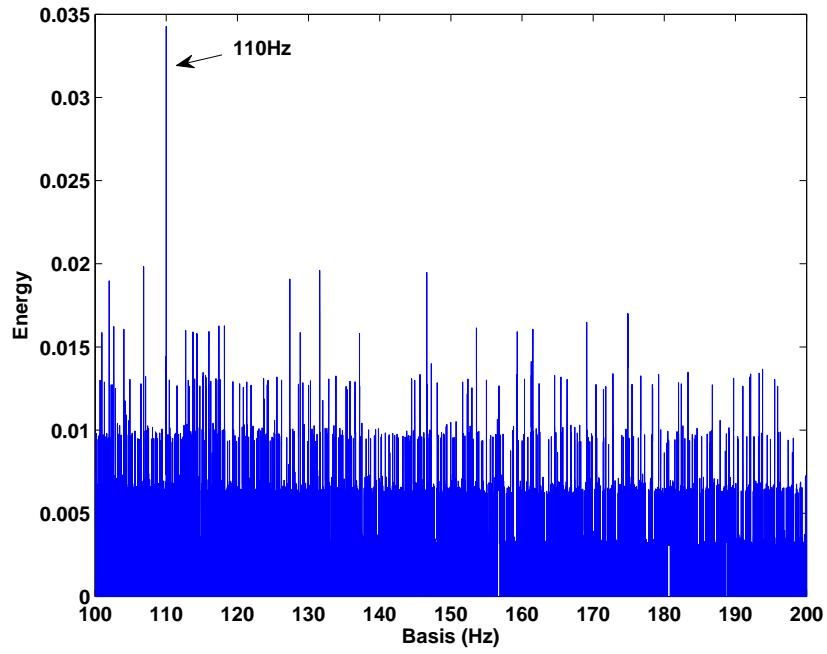


Figure 11: The SIOS of the simulated signal: $E(i)$ in case of (b).

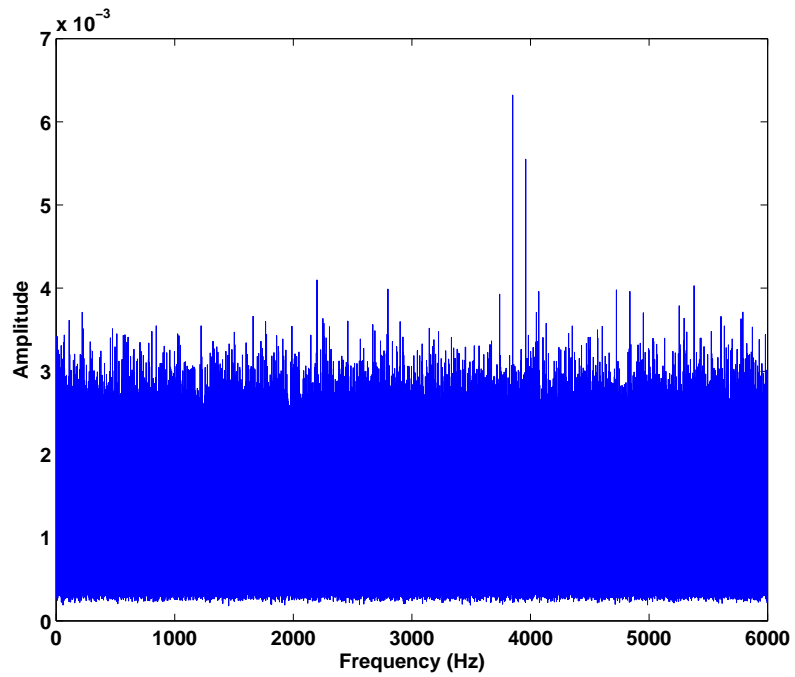


Figure 12: The spectrum of the simulated signal: case of (b).

Table 1: Bearing fault frequencies (multiple of running speed in Hz)

BPFO	BPMF	FTF	BSF
3.585	5.415	0.3983	2.357

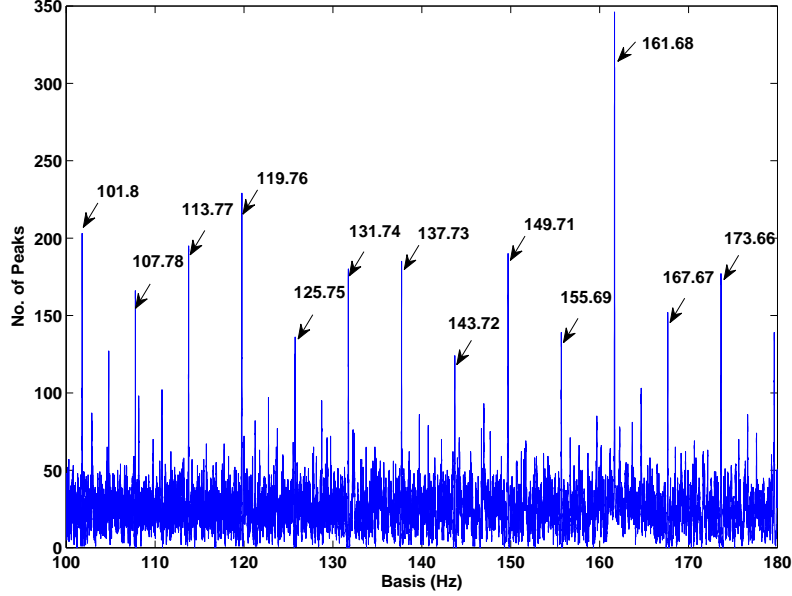


Figure 13: SIOS - $N(i)$ of Record 105 (1797rpm), inner-race fault.

105, 130, 118 as examples to demonstrate the results, which are with inner-race fault, outer-race fault and ball fault respectively.

Fig. 13 and 14 depict the SIOS of record 105 with inner-race fault. The dominant component can be easily identified on the basis, which is 161.68Hz. It is clearly corresponding to the inner-race fault ($1 \times \text{BPMF}$). Fig. 15 and 16 depict the SIOS of record 130 with outer-race fault. The dominant component can also be easily identified on the basis, which is 107.65Hz. It is clearly corresponding to the outer-race fault ($1 \times \text{BPFO}$).

It is interesting that, all significant components in Fig. 13 and 15 seem to be harmonics of $0.2 \times f_r$. Similar observations have been found in [15] when records with ball fault were analyzed with the envelope spectrum. As stated in [15], it is quite likely that the amount of mean slip in bearing has adjusted itself to lock onto an exact subharmonic of a dominant frequency such as shaft speed. In this case BPMF seems to lock onto $5.4 \times$ and BPFO seems to lock onto $3.6 \times$, which are both multipliers of $0.2 \times$. This is also confirmed by most of records with inner-race fault or outer-race fault, whose harmonics of $0.2 \times$ are significant on the SIOS and the component corresponding to $5.4 \times$ or $3.6 \times$ is the dominant one in $N(i)$ and $E(i)$ of the SIOS.

Fig. 17 and 18 depict the SIOS of record 118 with ball fault. An interesting

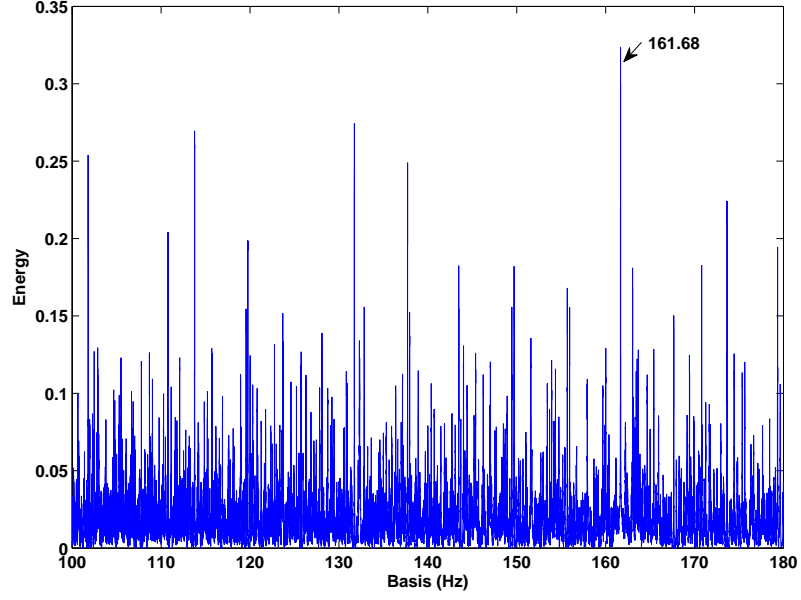


Figure 14: SIOS - $E(i)$ of Record 105 (1797rpm), inner-race fault.

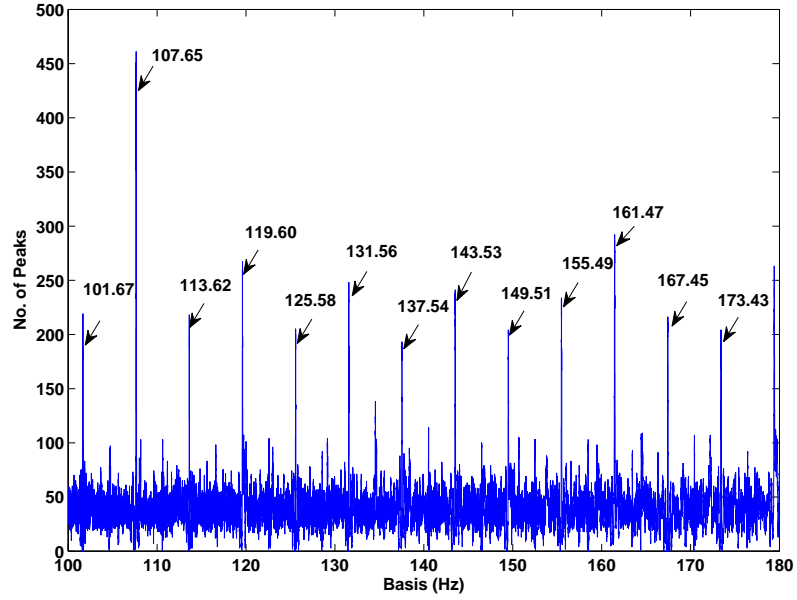


Figure 15: SIOS - $N(i)$ of Record 130 (1797rpm), outer-race fault.

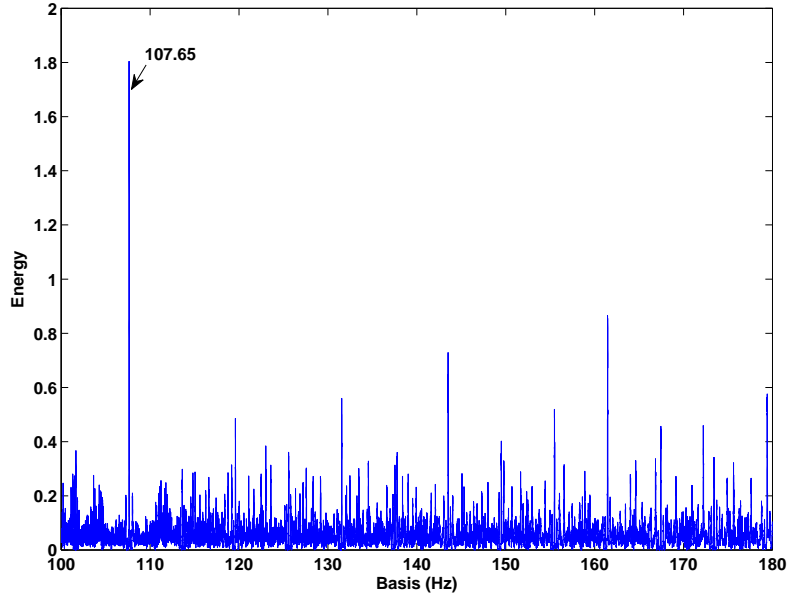


Figure 16: SIOS - $E(i)$ of Record 130 (1797rpm), outer-race fault.

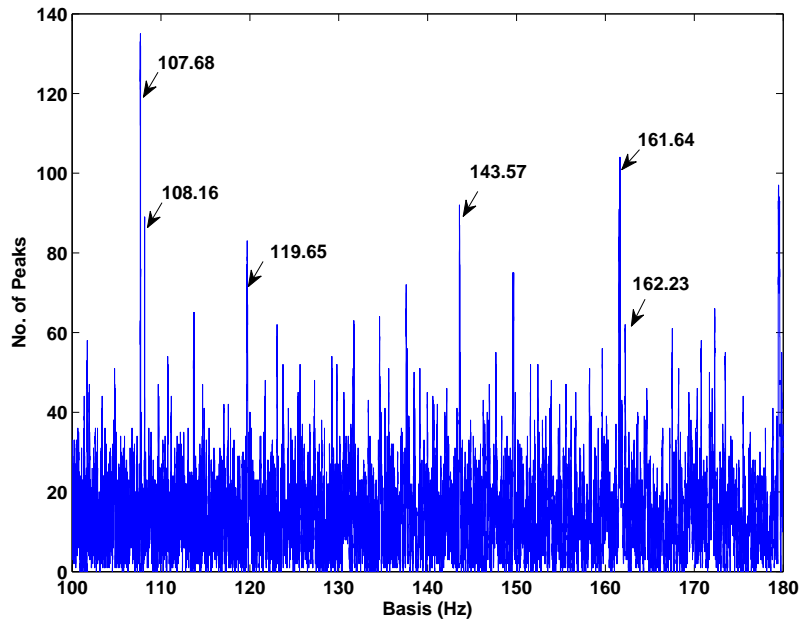


Figure 17: SIOS - $N(i)$ of Record 118 (1796rpm), ball fault.

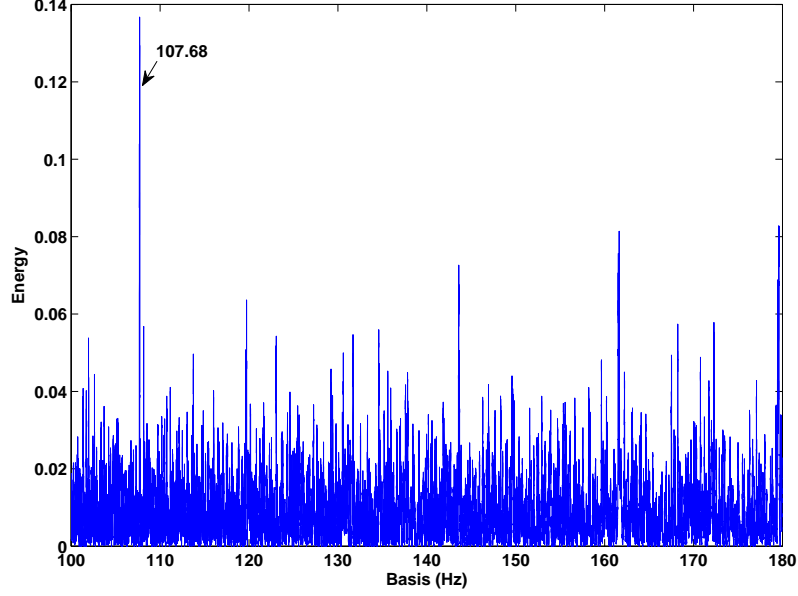


Figure 18: SIOS - $E(i)$ of Record 118 (1796rpm), ball fault.

feature is that the ball fault records often present evidence of outer and inner race faults, which was also discussed in [15]. Most of the marked components in Fig. 17 are harmonics of $0.2\times$, among which 107.68Hz is related to $3.6\times$ (BPFO) and 143.57Hz is related to $2.4\times$ (BSF) and 119.65 is related to $0.4\times$ (FTF). Nevertheless the components with 162.23Hz and 108.16Hz are harmonics of $0.2006\times$ other than $0.2\times$. The component with 162.23Hz is related to $5.416\times$ (BPFI). It is worth mentioning the ball fault pattern (BFP) composed of $3.6\times f_r$, $5.416\times f_r - 9\times 0.2006\times f_r$, $3.6\times f_r + 9\times 0.2\times f_r$ and $5.416\times f_r$ (like 107.68Hz, 108.16Hz, 161.64Hz and 162.23Hz in Fig. 17) exists in records 118-121, 185-188 and 222-225. The significant components with $4.8\times$ ($2\times$ BSF) and $4\times$ ($10\times$ FTF) exist in most records with ball fault except record 3005 - 3008. In fact the dominant component in record 3005 - 3008 is $4.714\times$ ($2\times$ BSF) shown in Fig. 19 and 20. It seems that there is no slip of characteristic frequencies in record 3005 - 3008.

Based on above analysis, the bearings are diagnosed based on the SIOS according to the following rules:

- inner-race fault: the dominant component in SIOS is $\text{BPFI} \times f_r$,
- outer-race fault: the dominant component in SIOS is $\text{BPFO} \times f_r$, and
- ball fault: the BFP, $2\times\text{BSF}$, and at least one harmonic of FTF are significant in SIOS; or $2\times\text{BSF}$ is dominant in SIOS.

The diagnosis results are compared with the benchmark study in [15], where envelope analysis, spectral kurtosis and cepstrum techniques were applied. As listed in Table B2 given by [15], record 171 with inner-race fault are relatively

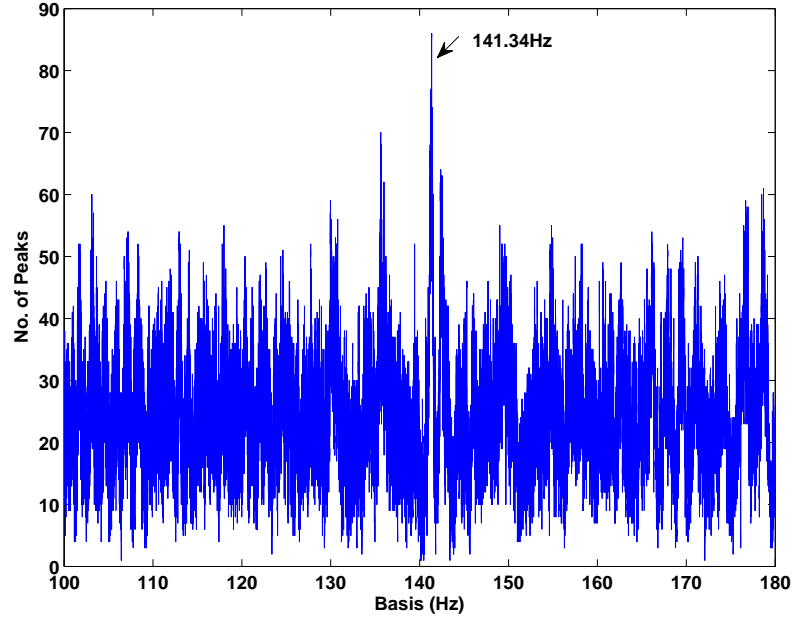


Figure 19: SIOS - $N(i)$ of Record 3005 (1797rpm), ball fault, $\sigma = 0.002$.

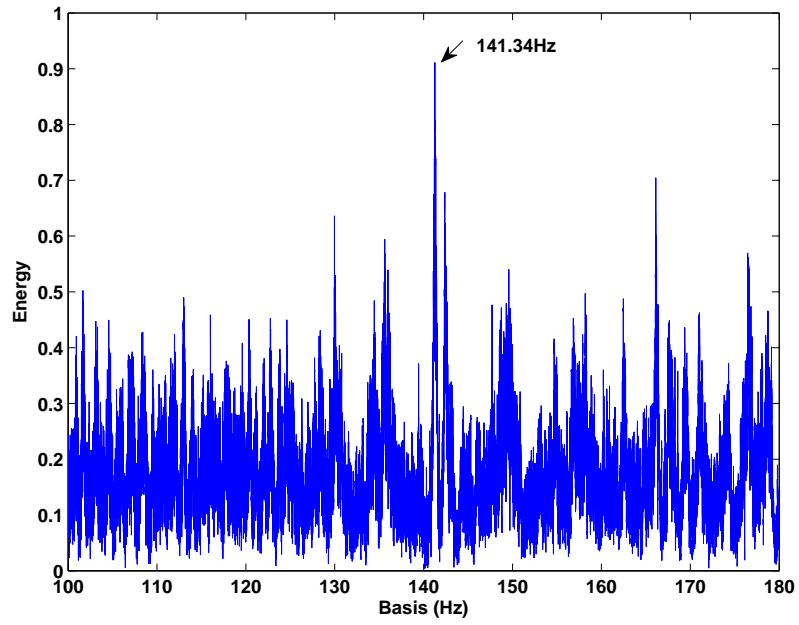


Figure 20: SIOS - $E(i)$ of Record 3005 (1797rpm), ball fault, $\sigma = 0.002$.

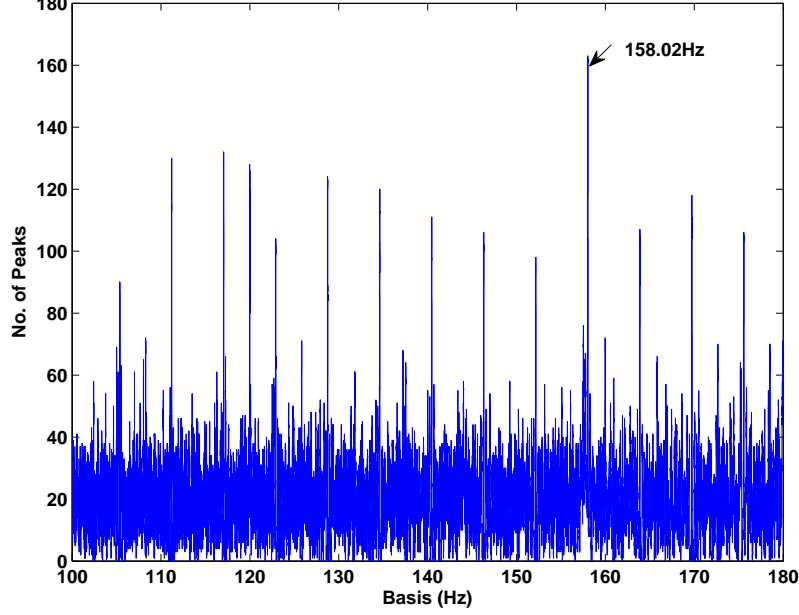


Figure 21: SIOS - $N(i)$ of Record 171 (1750rpm), inner-race fault.

difficult to diagnose, and record 197, 198, 199, 200 with outer-race fault can not be diagnosed or only partly diagnosed through the benchmark method. Besides, most of DE records with ball fault can not be well diagnosed in [15]. We take record 171, 197 and 224 to illustrate the effectiveness of the proposed method, and Table 2 - Table 4 give the full diagnosis results with the proposed method and the benchmark results. Record 121 and 188 with ball fault can not be fully diagnosed, where the BFP can not be fully identified and $2 \times \text{BSF}$ is not dominant in the SIOS. With the proposed method satisfied results can also not be obtained for record 3001-3004, and the reason is similar with that demonstrated in [15].

4 Discussion

4.1 About the identification of sidebands based on SIOS

It is known that there should be sidebands spaced at f_r around $\text{BPFO} \times$ in case of inner-race faults and sidebands spaced at FTF around $\text{BSF} \times$ in case of ball faults. In [15] classical sidebands was found in some of the CRWU bearing data, especially in records with inner-race fault.

The proposed method can also effectively identify the sidebands around interested frequencies, e.g. $\text{BPFI} \times$, $\text{BSF} \times$ and $\text{BPFO} \times$. Firstly $\text{BPFI} \times$, $\text{BSF} \times$ and $\text{BPFO} \times$ can be detected by looking at the dominant component of the SISO as described in the last section, and then a new basis can be defined with the range determined by the possible sidebands, e.g. 30Hz for detecting sidebands

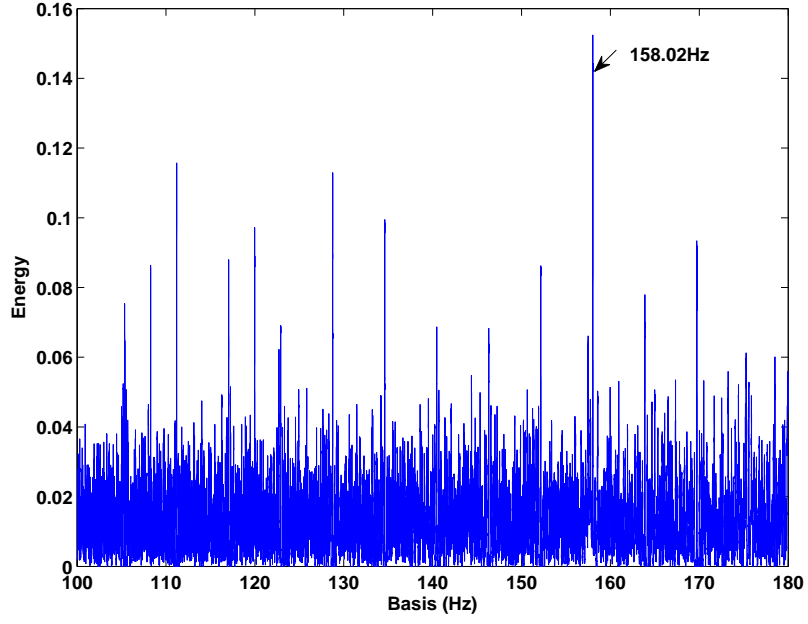


Figure 22: SIOS - $E(i)$ of Record 171 (1750rpm), inner-race fault.

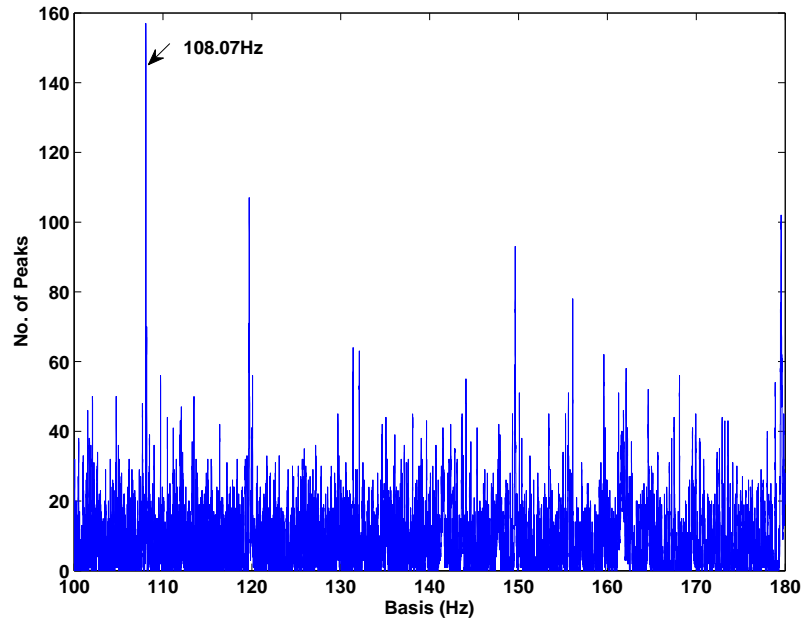


Figure 23: SIOS - $N(i)$ of Record 197 (1797rpm), outer-race fault.

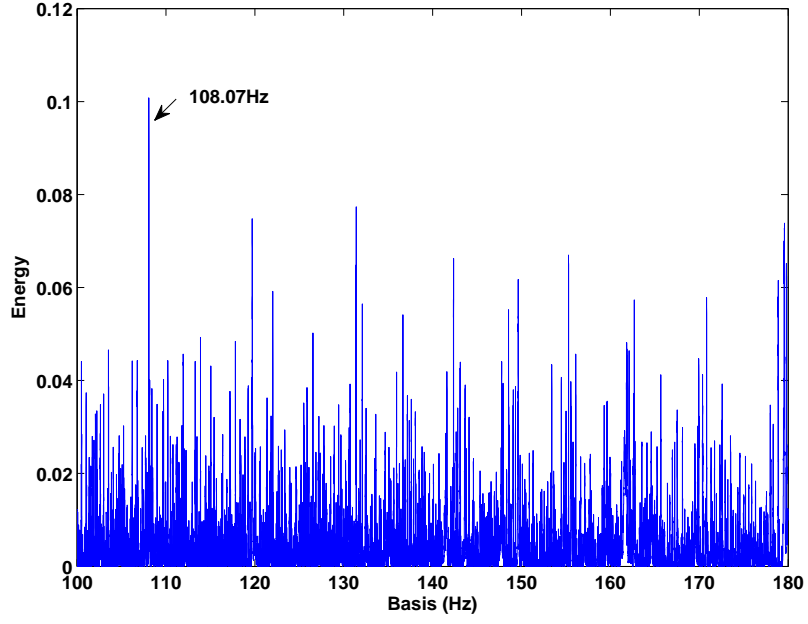


Figure 24: SIOS - $E(i)$ of Record 197 (1797rpm), outer-race fault.

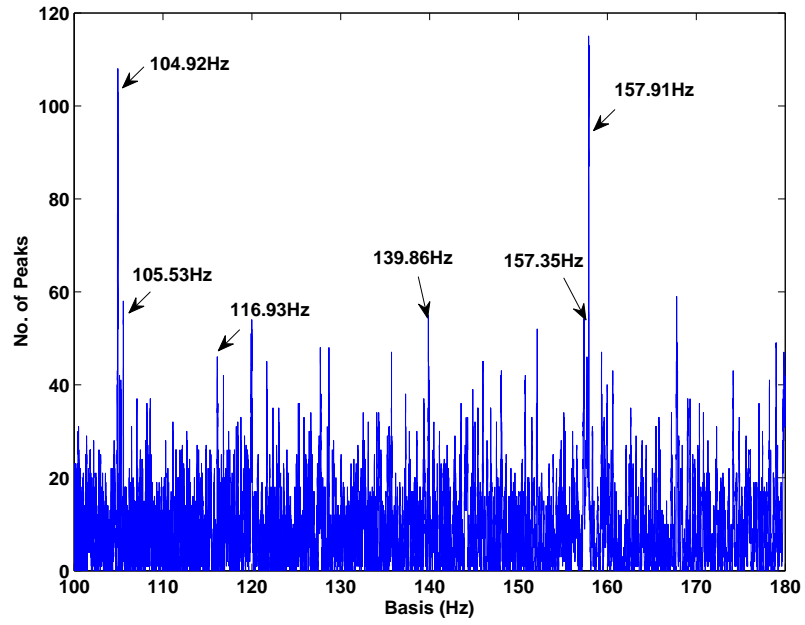


Figure 25: SIOS - $N(i)$ of Record 224 (1754rpm), ball fault.

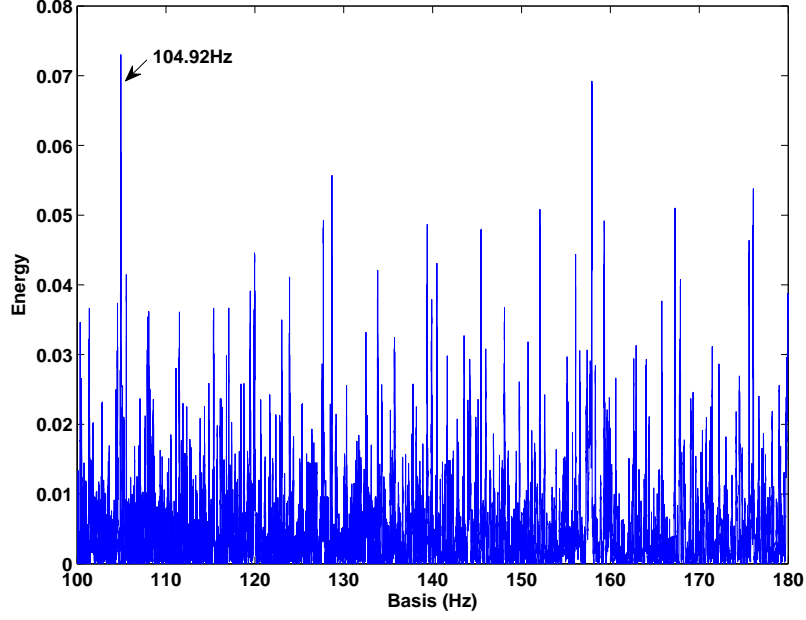


Figure 26: SIOS - $E(i)$ of Record 224 (1754rpm), ball fault.

Table 2: 12K drive end bearing fault analysis results: Inner-race fault. DE only.
Y=successful, P=partially successful, N=not successful

Inner-race faults		
Data Set	Diagnosis Result	Benchmark Result (M1,M2,M3)
105	Y	Y,-,-
106	Y	Y,-,-
107	Y	Y,-,-
108	Y	Y,-,-
169	Y	Y,Y,Y
170	Y	Y,Y,Y
171	Y	Y,Y,Y
172	Y	Y,Y,Y
209	Y	Y,-,-
210	Y	Y,-,-
211	Y	Y,-,-
212	Y	Y,-,-
3001	N	N,N,N
3002	N	N,N,N
3003	N	N,N,N
3004	N	N,N,N

Table 3: 12K drive end bearing fault analysis results: Outer-race fault. DE only. Y=successful, P=partially successful, N=not successful

Outer-race faults		
Data Set	Diagnosis Result	Benchmark Result (M1,M2,M3)
130	Y	Y,-,-
131	Y	Y,-,-
132	Y	Y,-,-
133	Y	Y,-,-
197	Y	N,N,Y
198	Y	P,N,N
199	Y	P,N,N
200	Y	N,N,N
234	Y	Y,-,-
235	Y	Y,-,-
236	Y	Y,-,-
237	Y	Y,-,-

Table 4: 12K drive end bearing fault analysis results: Ball fault. DE only. Y=successful, P=partially successful, N=not successful

Ball faults		
Data Set	Diagnosis Result	Benchmark Result (M1,M2,M3)
118	Y	N,N,N
119	Y	N,N,N
120	Y	N,N,P
121	P	N,P,P
185	Y	P,P,P
186	Y	P,P,P
187	Y	P,N,P
188	P	P,P,P
222	Y	P,Y,Y
223	Y	Y,Y,Y
224	Y	N,N,P
225	Y	N,N,P

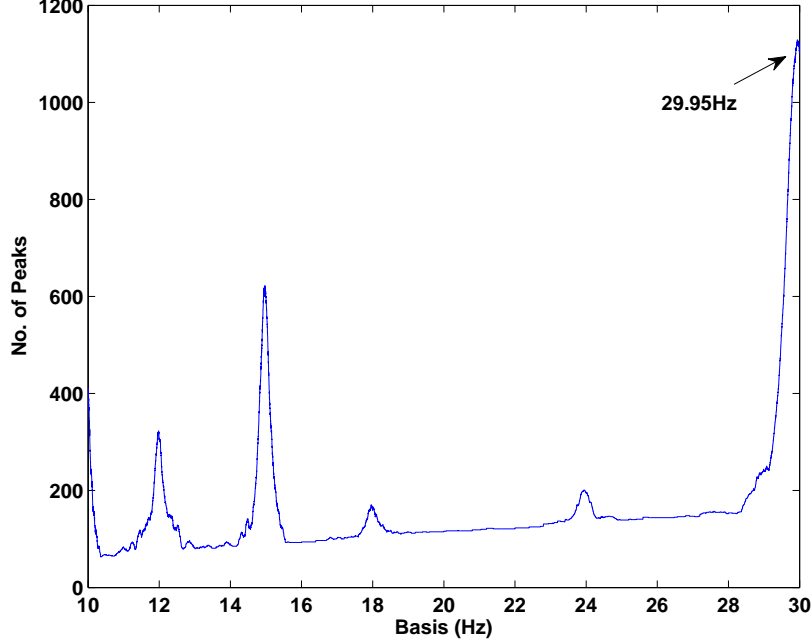


Figure 27: Sideband identification - $N(i)$ of Record 105 (1797rpm), inner-race fault.

spaced at f_r ($< 29.95\text{Hz}$) and sidebands spaced at FTF ($< 12\text{Hz}$) in the CRWU bearing data [14]. Then we can locate local peaks, i.e. $P(k)$, to the i th bin of the new basis according to

$$|F(k) - \beta_j f_{do}|/B(i) - \lfloor |F(k) - \beta_j f_{do}|/B(i) \rfloor < \sigma,$$

$$\beta_j f_{do} - R/2 \leq F(k) \leq \beta_j f_{do} + R/2$$

where f_{do} represents the characteristic frequencies ($\text{BPFI}\times$, $\text{BSF}\times$ or $\text{BPFO}\times$) and R is the width of the new basis.

Fig. 27, 28 and 29 show the sidebands of records 105, 130 and 118 respectively. The dominant component in Fig. 27 is 29.95Hz which is f_r , and the dominant component in Fig. 29 is 23.8Hz which is $2\text{FTF}\times$. They are typical signatures [15]. Nevertheless dominant sidebands are also identified in records with outer-race fault, i.e. record 130. Also $\text{FTF}\times$ is found in Fig. 27 in case of inner-race fault, and more complicate sidebands are shown in Fig. 29 in case of ball fault. That means the vibration of bearings are complex and other mechanical defects may exist [15], but the dominant sidebands still provide strong evidence of the main fault of bearings.

4.2 About the selection of l and δ in Eq. (2)

According to Eq. (2), the number of local peaks is determined by the selection of l and δ . Since the average power in different frequency bands may be

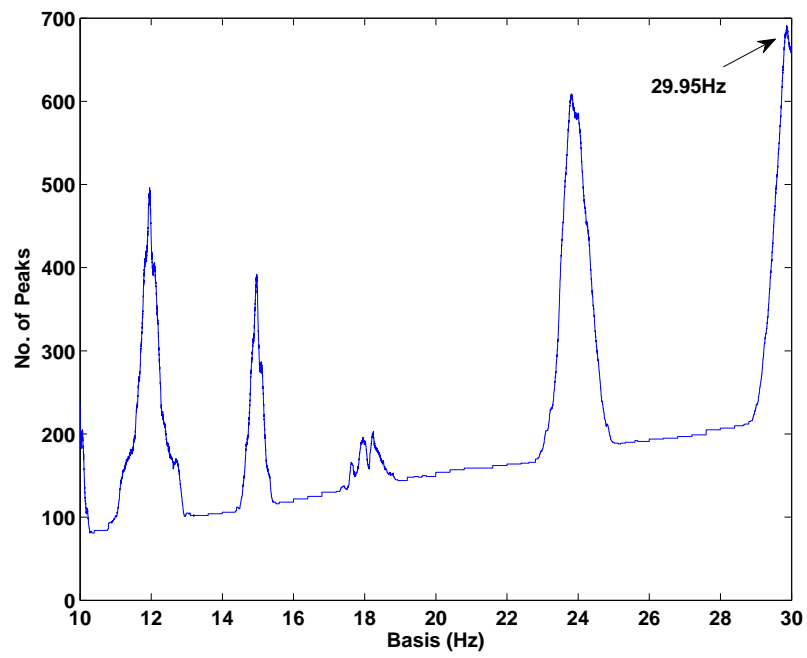


Figure 28: Sideband identification - $N(i)$ of Record 130 (1797rpm), outer-race fault.

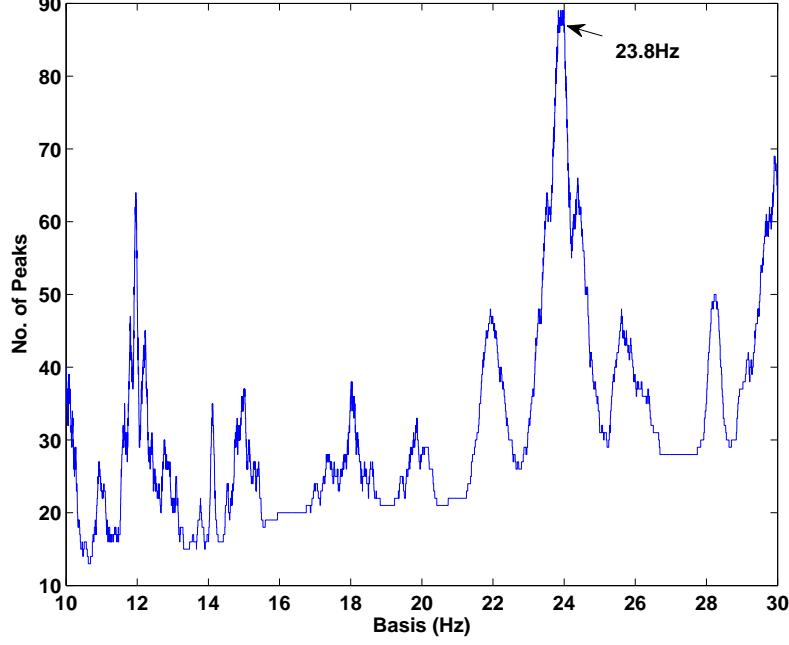


Figure 29: Sideband identification - $N(i)$ of Record 118 (1796rpm), ball fault.

varying, we use l in Eq. (2) to build a frequency-dependent baseline in order to suppress frequency bins with low power amplitudes. The selection of l is not strict, and it can be simply chosen such that $2l + 1$ bins represent any desired frequency bandwidth, e.g. 50Hz, 100Hz. Then the number of local peaks will be controlled through the selection of δ . If δ is too small, then only a few local peaks can be found and therefore some harmonics may be lost. If δ is too large, the number of local peaks could be large and the searching effort could be very high. Since the harmonics of bearing characteristic frequencies usually have relatively larger amplitudes, in practice we suggest to select δ such that 0.5% \sim 3% of amplitudes are treated as local peaks.

In the benchmark study l is set as 10000, such that the bandwidth of 114Hz is used to compute the moving average. And δ is set as 0.0002 for most records except record 3005-3008. Since the spectrums of different loads and different faults (with different sizes) are quite different, in fact 0.5% \sim 2.1% of amplitudes are treated as local peaks in the SIOS of different spectrums with the same l and δ . From this point of view, the use of the same parameters for those different spectrums have already demonstrated that l and δ are not sensitive to the construction of the SIOS if they are within a reasonable range.

4.3 About the determination of the basis

If the characteristic frequencies of a given type of bearings are roughly estimated according to the geometrical parameters, the basis B can be selected as the range of estimated characteristic frequencies. If the characteristic frequen-

cies are unknown, the basis B could also be with any range. There is no any restriction on the selection of B except $F_l > 1\text{Hz}$, which can be easily satisfied. When $F_h < 2F_l$, $F(k)$ is located on only one bin of B ; Otherwise some local peaks may be located on more than one bin of B .

4.4 Advantages and limitations

The proposed method is based on a simple searching algorithm, and it is effective in finding the harmonics of the interested frequency range. Even the harmonics with small amplitudes could be found and located on the basis. Although noises and other random impulses may introduce some local peaks unrelated to the faults, the significant components in the SIOS can still be clearly recognized and related to the characteristic frequencies of bearing. The proposed method is robust against noises and random impulses, and it is still effective when noise and smearing are heavy. Similar methods, e.g. cepstrum, usually could not find enough periodic components of the signal in case of heavy noises and other interferences. As illustrated in the benchmark study of bearings, the proposed method could provide more information about the harmonics of impulses than the envelop analysis in [15] and better diagnosis results can be achieved. Besides, the assumption 1 of the method can generally be satisfied, and there is no other further restriction of the method.

Limitations of the proposed method are as follows: (a) the SIOS can only provide qualitative information, where $N(i)$ and $E(i)$ are not the true value due to the finite spectrum resolution and noises; (b) the computation effort could be high, when the range of the basis or the number of local peaks is large.

5 Conclusion

A simple and effective method for detecting bearing faults has been proposed based on a searching algorithm. The SIOS of vibration signals was constructed, such that the information of the train of harmonics was clearly represented with $N(i)$ and $E(i)$ on a defined basis. The dominant components of the SIOS were corresponding to the characteristic frequency of bearings, and the sidebands of those characteristic frequencies could also be identified. Based on the SIOS faults of bearings were successfully diagnosed. Its effectiveness was verified with simulated bearing signals and the benchmark results.

Acknowledgements

The research is supported by National Natural Science Foundation of China (51475455), and the Project Funded by the Priority Academic Program Development of Jiangsu Higher Education Institutions(PAPD).

References

- [1] H. Zoubek, S. Villwock, and M. Pacas, Frequency response analysis for rolling bearing damage diagnosis, *IEEE Trans. Ind. Electron.*, 55 (2008) 4270-4276.
- [2] R.B. Randall, and J. Antoni, Rolling element bearing diagnosticsA tutorial, *Mechanical Systems and Signal Processing*, 25 (2011) 485-520.

- [3] A.K.S. Jardine, D. Lin, D. Banjevic, A review on machinery diagnostics and prognostics implementing condition-based maintenance, *Mechanical Systems and Signal Processing*, 20 (2006) 1483-1510.
- [4] M.F. Abdel-Magied, K.A. Loparo, and L. Wei, Fault detection and diagnosis of rotating machinery, *IEEE Trans. Ind. Electron.*, 47 (2000) 1005-1014.
- [5] D. Bently, Predictive Maintenance Through the Monitoring and Diagnostics of Rolling Element Bearings, Bently Nevada Co., pp. 2-8, 1989. Application Note 44.
- [6] N. Li, R. Zhou, Q. Hu, and X. Liu, Mechanical fault diagnosis based on redundant second generation wavelet packet transform, neighborhood rough set and support vector machine, *Mechanical Systems and Signal Processing*, 28 (2012) 608-621.
- [7] Y. Lei, J. Lin, Z. He, and M.J. Zuo, A review on empirical mode decomposition in fault diagnosis of rotating machinery, *Mechanical Systems and Signal Processing*, 35 (2013) 108-126.
- [8] J. Antoni, The spectral kurtosis: a useful tool for characterising non-stationary signals, *Mechanical Systems and Signal Processing*, 20 (2006) 282-307.
- [9] D. Wang, P.W. Tse, K.L. Tsui, An enhanced Kurtogram method for fault diagnosis of rolling element bearings, *Mechanical Systems and Signal Processing*, 35 (2013) 176-199.
- [10] Y. Lei, J. Lin, Z. He, and Y. Zi, Application of an improved kurtogram method for fault diagnosis of rolling element bearings, *Mechanical Systems and Signal Processing*, 25 (2011) 1738-1749.
- [11] W. Su, F. Wang, H. Zhu, Z. Zhang, and Z. Guo, Rolling element bearing faults diagnosis based on optimal Morlet wavelet filter and autocorrelation enhancement, *Mechanical Systems and Signal Processing*, 24 (2010) 1458-1472.
- [12] Y. Wang, and M. Liang, An adaptive SK technique and its application for fault detection of rolling element bearings, *Mechanical Systems and Signal Processing*, 25 (2011) 1750-1764.
- [13] Y. Zhang, and R.B. Randall, Rolling element bearing fault diagnosis based on the combination of genetic algorithms and fast kurtogram, *Mechanical Systems and Signal Processing*, 23 (2009) 1509-1517.
- [14] Bearing Data Center, Case Western Reserve Univ., Cleveland, OH. [Online]. Available: <http://www.eecs.case.edu/laboratory/bearing>
- [15] W. Smith, R.B. Randall, Rolling element bearing diagnostics using the Case Western Reserve University data: A benchmark study, *Mechanical Systems and Signal Processing*, 64-65 (2015) 100-131.